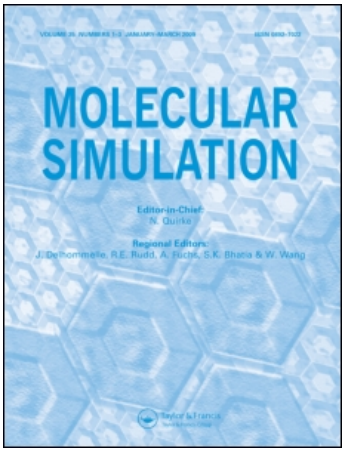

Molecular Simulation
Publication details, including instructions for authors and subscription information:
http://www.informaworld.com/smpp/title~content=t713644482

Valence orbital response to conformers of *n*-butane

F. Wang[a]; W. Pang[b]
[a] Centre for Molecular Simulation, Swinburne University of Technology, Melbourne, Victoria, Australia [b] Polarization Physics Laboratory, Department of Physics, Tsinghua University, Beijing, P. R. China

To cite this Article Wang, F. and Pang, W.(2007) 'Valence orbital response to conformers of *n*-butane', Molecular Simulation, 33: 14, 1173 — 1185
To link to this Article: DOI: 10.1080/08927020701504137
URL: http://dx.doi.org/10.1080/08927020701504137

Molecular Simulation, Vol. 33, No. 14, December 2007, 1173–1185

Taylor & Francis
Taylor & Francis Group

Valence orbital response to conformers of *n*-butane

F. WANG†* and W. PANG‡

†Centre for Molecular Simulation, Swinburne University of Technology, PO Box 218, Hawthorn, Melbourne, Victoria 3122, Australia
‡Polarization Physics Laboratory, Department of Physics, Tsinghua University, Beijing 100084, P. R. China

(Received April 2007; in final form June 2007)

Individual outer valence orbital responses to rotations of the C—C central bond of butane (C_4H_{10}) are explored on the torsional potential energy surface. Orbital ionization energies, topologies and momentum distributions for the four most significant butane conformation are presented, as snapshots of the conformational variations. The analysis is based on quantum mechanically generated information from coordinate space and momentum space, a technique called dual space analysis (DSA). By comparison with experimental measurements of photo-electron spectra (PES) for energies and of electron momentum spectra (EMS) for energies and Dyson orbitals, we demonstrate that the individual outer valence orbitals of these conformers response differently to the rotations of the central C—C bond of *n*-butane. Orbital signatures of other higher energy conformations, such as orbitals $1a_2$ and $5a_1$ of conformation D (C_{2v}), are identified. This finding indicates a co-existence of butane conformations, although the global minimum structure of anti-butane, A (C_{2h}), is dominant. Orbital topology and electron charges redistribution during the transformation provide useful information on the chemical bonding and related chemical reactions.

Keywords: Dual space analysis; *n*-butane conformational analysis; Electron momentum spectroscopy; Valence orbital responses; Density functional theory calculations

1. Introduction

Many organic and biomolecules with single bonds, such as butane (C_4H_{10}), are subject to conformational effects. Conformations which likely exist under the experimental conditions [1–4] are reasonable for as large as 0.2 eV energy difference in their first ionization energies [2–4]. As a prototype for its conformations [5], summaries of recent work on butane appear in Refs. [1,6–10]. Of the four rotational isomers (or rotamers) of butane, only anti-butane (structure A with a point group symmetry C_{2h}) and gauche butane (structure C with a point group symmetry C_2) are stable species [11,12] as they possess energy minima on the torsional potential surface. Structures B—eclipsed-butane, barrier, $\delta \approx 60°$—and D—*cis*-butane, $\delta = 180°$—are considered as transition structures. When one states a particular conformer to be more stable than another, one does not mean that the molecule in question adopts and maintains only the more stable conformation [11]. Near 300 K, sufficient thermal energy is present to ensure that rotation about σ bonds occurs rapidly and that all possible conformers are in a fluid equilibrium based on a Boltzmann distribution. When a reaction is exothermic, initial interaction of frontier molecular orbitals (MOs) generally leads to the expected products; for endothermic reactions, information with respect to the structure and stability of a transition state is necessary to specify the reaction pathway [5].

As a simple alkane that has attracted considerable research attention [13–15], butane has a structure that had been considered to be firmly established and fully understood [7,9]. However, this conclusion was seriously challenged in the past decade by experiments such as electron momentum spectroscopy (EMS) [16–19]. For example, calculations of the binding energies [9,20,21] of electrons in saturated hydrocarbons of varying size and complexity have shown that a mixture of carbon 2s2p plus hydrogen 1s atomic orbitals (AOs) is involved in both inner and outer valence shells in a range of 14–22 eV. Hence there is a long-range interaction and strong dependence of the binding-energy spectra on the conformation of chains [9]. Limited instrumental resolution in the experiments yields clusters of unresolved orbitals in the outer valence shell in the EMS measurement [16,17] that might result in loss of information in the most chemically significant region [8].

Photo-electron spectra (PES) [12] are capable of greater resolution in binding-energy spectra, but assignment of

*Corresponding author. Fax: +61-3-9214-5075. Email: fwang@swin.edu.au

Molecular Simulation
ISSN 0892-7022 print/ISSN 1029-0435 online © 2007 Taylor & Francis
http://www.tandf.co.uk/journals
DOI: 10.1080/08927020701504137

their features (spectral peaks) in the often congested binding-energy spectra to the orbitals of a molecule [22] is ambiguous. For this reason, PES relies on theoretical calculations to aid assignments [12], but these might depend on a theoretical model if it is insufficiently accurate. For instance, PES of butane [12] were assigned based on RHF/4-21G* calculations with a reduced symmetry corresponding to a point group symmetry C_s, which describes unsatisfactorily the ground-state configuration ($X\,^1A_g$) with a point group symmetry C_{2h} applicable to the global minimum structure. Experiments generally provide values of properties of conformers vibrationally averaged over thermal motions, whereas theoretical calculations can produce results for the equilibrium states of a specific species [23].

An important objective in investigating molecular electronic structure is the mechanism of chemical bonding, which is fundamental to an understanding of reactivity, particularly in organic chemistry. Dyson orbitals indicate the orbital-based bonding characteristics that directly contribute to mechanisms of chemical bonding [24]. A σ-bond or a π-bond in a molecule depends on both the angular momenta of the component orbitals and the manner of bonding, i.e. the projection of the total angular momentum. For example, p-AOs can form either σ-bonds or π-bonds. Some bonds exhibit mixed contributions from s-AOs and p-AOs, as "hybrid bonds". In *k*-space, the dependence of orbital angular momentum is correlated with binding-energy spectra and with distributions of orbital momentum [25]. Hence, from orbital MDs with information about the molecular point group symmetry and from distributions of orbital-electron density, the bonding nature can be deduced unambiguously, which makes such combined information in both *r*-space and *k*-space particularly useful to identify the orbital-based fingerprints of isomers [1,2,6,26,27].

In a systematic calculation for butane based on a CCSD(T) level of theory [7], anti-butane (A) is associated with the global minimum located with 0.62 kcal mol^{-1} below the local minimum conformation due to the gauche (C) conformer obtained on torsional rotation about the central C—C bond. The electronic structure of butane, results in differences in vertical ionization energies and the outer valence orbital topology of its conformations in the course of torsional motions [9,28]. Based on our previous experience of butane (C_{2h}, global minimum structure) [8], on the core orbitals [6] and the inner valence orbitals [1], we employed dual space analysis (DSA) [8] to demonstrate in the present work that the outer valence Dyson orbitals response differently to the conformational changes. The present work also demonstrates that DSA is a useful alternative to the analysis of temperature dependence of specific rotation of conformations [29,30].

2. Binding energy spectra of butane conformations

Computational details of the present work are similar to those in Ref. [8], that is, the electronic calculations were performed using a B3LYP/TZVP//MP2/TZVP model with the Gamess-US02 [31] program. The basis set is the DGauss DFT due to Godbout *et al.* [32]. The vertical ionization energies of the conformations were generated using a DFT model with $V_{xc} = SAOP$ [33–36], base on the "*meta*-Koopman" approximation available in the Amsterdam density functional (ADF) suite [37]. The connection between Kohn–Sham (KS) orbitals and Dyson orbitals allows the spin-unrestricted KS exchange-correlation potential (V_{xc}) to be expressed as statistically averaged individual V_{xc} potentials for Dyson spin-orbitals as the leading term [38].

Conformations of butane have the same order of attachment of atoms but diverse spatial arrangements caused by rotation about single bonds [5]. Although conformers are typically difficult to isolate, a particular conformer is likely to be more stable than any other; the dominant conformer therefore generally pertains to the most stable conformation. In the most stable structure, anti-butane (A, C_{2h}), a plane of symmetry contains all skeletal carbon atoms. The principal rotational axis, C_2, is the *z*-axis which is perpendicular to that plane *xy*. When the central C—C bond rotates, the symmetry plane is lost but the principal C_2-axis is retained. When the torsional angle, δ, rotates 180°, the structure of anti-butane becomes *cis*-butane (D) belonging to a point group symmetry C_{2v}, which is the least stable structure of butane (figure 1) on the torsional potential-energy surface. As butane rotates around its C—C central bond, the principal rotational axis, C_2, rotates accordingly within the *yz*-plane; as a result, for

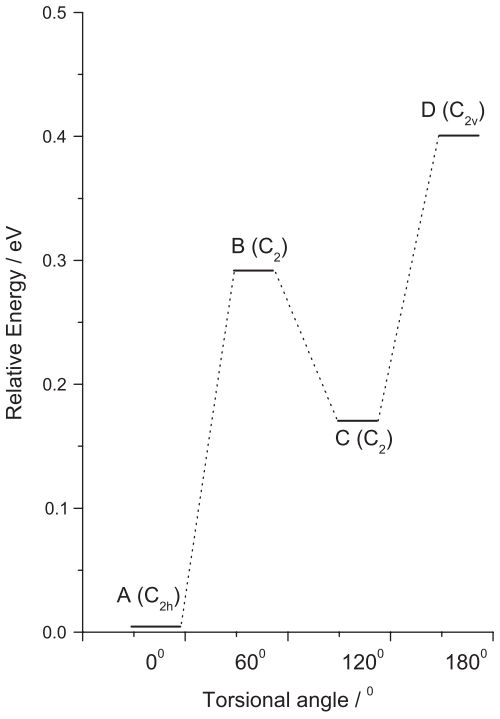

Figure 1. Relative energies of butane conformers on the torsional potential-energy surface; data are based on SAOP/TZ2P//MP2/TZVP calculations.

anti-butane, A, the C_2 axis is the z-axis, but, when the rotation produces *cis*-butane, D, the C_2 axis becomes the y-axis as if it were in the A structure. In such a rotational process, the C_2 subgroup is retained, which exerts an impact on the orbital topology of the conformations.

The configurations of butane conformations in the ground electronic state can not be directly deduced from either EMS or PES experiment, but can be determined based on quantum-mechanical calculations [12,16,17]. The electronic configurations depend on the models and inclusion of the V_{xc} energy. In the outer valence shell, orbitals possess small differences in orbital energy; correlation energies of the same magnitude might, hence, alter the ordering of orbital energies (configuration). According to our B3LYP/TZVP//MP2/TZVP calculations, the outer valence-shell electronic configurations for the conformers are

A: anti-butane (C_{2h}, $X\,^1A_g$):
$(1a_u)^2(5a_g)^2(5b_u)^2(1b_g)^2(6b_u)^2(2a_u)^2(6a_g)^2(2b_g)^2(7a_g)^2$
B: eclipsed-butane (C_2, $X\,^1A$):
$(5a)^2(5b)^2(6a)^2(6b)^2(7a)^2(7b)^2(8a)^2(8b)^2(9a)^2$
C: gauche-butane (C_2, $X\,^1A$):
$(5b)^2(5a)^2(6a)^2(6b)^2(7a)^2(7b)^2(8a)^2(8b)^2(9a)^2$
D: *cis*-butane (C_{2v}, $X\,^1A_1$):
$(1b_1)^2(5a_1)^2(1a_2)^2(6a_1)^2(5b_2)^2(2b_1)^2(6b_2)^2(7a_1)^2(2a_2)$

in which configurations of the global minimum anti-butane A and the local minimum gauche butane C agree satisfactorily with the corresponding configurations of A and C generated with the HF/6–311G** model [9]. The relative energies of the conformers are depicted in figure 1, as snapshots of the distinct structures on the surface of torsional potential energy.

The vertical ionization energies of the four butane conformations were calculated using the RHF/TZVP//MP2/TZVP model and DFT with SAOP/TZ2P model, of which the latter is a Slater-type triple-zeta basis set, TZ2P [39]. Figure 2 shows a comparison between the experimental binding energies of butane, a high-level calculation using an expensive one-particle Green's function (GF)lp-GF/ADC(3)/6-311G** method [9] and our results. All theoretical results in this figure, including the GF calculations, are based on the global minimum structure of butane. The vertical ionization energies generated with the SAOP/TZ2P and the lp-GF/ADC(3)/6-311G** models agree satisfactorily in the outer valence shell with the PES experiment [12], except the highest occupied molecular orbital (HOMO). The MP2/TZVP model generally overestimate the ionization energies in this region. All theoretical methods in figure 2 overestimate the ionization energy of HOMO, indicating that this orbital might contain additional effects of electron correlation that were insufficiently included in the methods employed. Other effects such as orbital relaxation effects and zero point vibrational energy may also contribute to this discrepancy. As a consequence, ΔSCF method, which takes the energy difference between

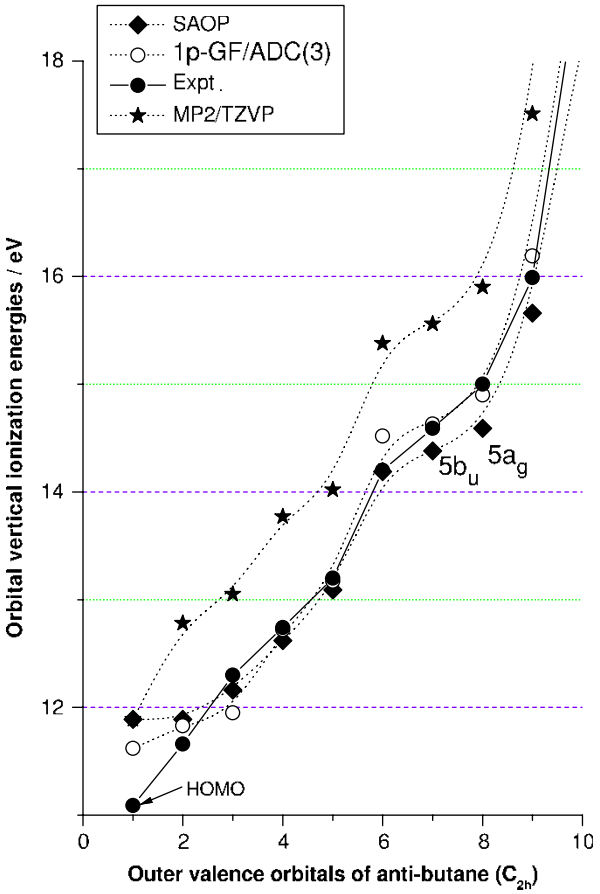

Figure 2. Comparison of vertical ionization energies of anti-butane, the global minimum energy structure of butane (A), between the present results from the SAOP/TZ2P and MP2/TZVP models, PES experiment [12] and 1p-GF/ADC(3)/6-311G** [9] results.

ground state of the neutral species and the ground state of its cation, may be further considered.

Table 1 presents the outer valence orbital vertical ionization energies of butane conformations of A, B, C and D with a comparison with Ip-GF/ADC(3)/6–311G** results (anti-butane A and gauche-butane C, only) [9], and with the available experimental EMS and PES data [12,16,17]. Due to instrumental resolution, the EMS measurement showed only four features in the binding-energy spectra [16,17]. The PES binding energies are better resolved in the outer valence energy region for anti-butane A. It should note that the experimentally observed binding energies are vibrationally averaged values of binding energies of all possible conformations in a Boltzmann distribution. The DFT SAOP/TZ2P model produced orbital ionization energies are in agreement with EMS and PES experimental measurements and with an accuracy competitive with the 1p-GF/ADC(3)/6-311G** model [9], for both minimal energy structures the C_{2h} and C_2 conformers. Note that the largest discrepancy between EMS and PES experiments is ca. 0.25 eV. The SAOP/TZ2P model is based on the MP2/TZVP geometry whereas the 1p-GF/ADC(3)/6-311G** model is based on the HF/6-311G** geometry [9]. Moreover, the HOMO and the next HOMO (NHOMO) of the anti-butane A conformer given by the SAOP/TZ2P

model are fortuitously degenerate in energy, and orbital $2b_g$ is the preferred HOMO in this model.

Figure 3 displays a correlation diagram of vertical ionization energies in the outer valence orbitals as a function of the torsional rotation, a snapshot of four butane conformations produced using the SAOP/TZ2P model (table 1). The nearly degenerate HOMO and NHOMO pair in conformer A splits in conformers B and C on rotation of the central C—C bond, but the orbital symmetries of *a* and *b* are maintained until *cis*-butane, $D(C_{2v})$, is produced. The HOMO/NHOMO orbital pair experiences a significant splitting when the structure is rotated to give *cis*-butane of D as shown in the last column of figure 3. The approximately 0.3 eV energy splitting in the HOMO–NHOMO for structure D inversely evidents that the HOMO of the global minimum structure A is $7a_g$ rather than $2b_g$. In addition, this diagram indicates that the NHOMO of conformation A, B and C (with symmetry *b*) do not lead to the NHOMO (symmetry *a*) but the third HOMO of structure D.

In this figure, all orbitals of *a*-symmetry are depicted in red and associated with red dashed lines to reveal the orbital topology. The outer valence orbitals of the conformers distributed in the energy region 11–16 eV exhibit disparate patterns. For conformations with a planar symmetry of the carbon skeleton such as A and D (both with a C_2-axis plus a symmetry plane), orbitals of the stable conformer (A) exhibit

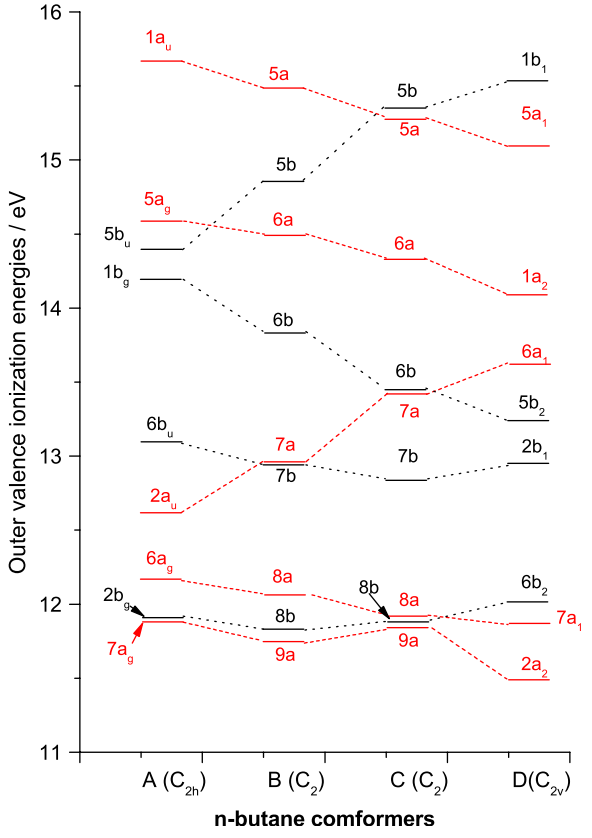

Figure 3. Orbital topology and correlation for the outer valence shell of four butane conformers; the SAOP/TZ2P model favours the $2b_g$ orbital as the HOMO.

Table 1. Comparison of orbital vertical ionization energies and symmetry of the *n*-butane conformers calculated using the RHF/TZVP and SAOP/TZ2P models with EMS, PES experiments and 1p-GF/ADC(3)/6-311G** calculations.

	Experiment		*Theoretical results*													
			$A(X^1A_g), C_{2h}$				$B(X^1A), C_2$			$C(X^1A), C_2$			$D(X^1A_1), C_{2v}$		
Peak no.	*EMS*[†]	*PES*[‡]	*sym*	*RHF*	*ADC(3)*[¶]	*SAOP*	*sym*	*RHF*	*SAOP*	*sym*	*RHF*	*ADC(3)*[¶]	*SAOP*	*sym*	*RHF*	*SAOP*
1	–	11.09	$7a_g$	12.41	11.62	11.89[§]	9a	12.36	11.75	9a	12.42	11.64	11.88	$2a_2$	12.12	11.48
2	11.57	11.66	$2b_g$	12.57	11.83	11.89[§]	8*b*	12.39	11.83	8*b*	12.47	11.71	11.87	$7a_1$	12.42	11.86
3	–	12.3	$6a_g$	12.74	11.95	12.16	8*a*	12.67	12.04	8*a*	12.59	11.83	11.93	$6b_2$	12.58	11.99
4	–	12.74	$2a_u$	13.49	12.72	12.62	7*b*	13.98	12.97	7*b*	13.73	12.91	12.84	$2b_l$	13.98	12.94
5	12.89	13.2	$6b_u$	14.02	13.17	13.09	7*a*	14.33	12.98	7*a*	14.44	13.54	13.44	$5b_2$	14.33	13.24
6	–	14.2	$1b_g$	15.46	14.52	14.19	6*b*	15.00	13.82	6*b*	14.54	13.67	13.44	$6a_1$	14.63	13.60
7	14.38	14.59	$5b_u$	15.62	14.63	14.38	6*a*	15.81	14.49	6*a*	15.64	14.65	14.33	$1a_2$	15.40	14.08
8	–	15.0	$5a_g$	15.91	14.90	14.59	5*b*	16.32	14.86	5*a*	16.84	15.74	15.28	$5a_1$	16.64	15.09
9	15.71	15.99	$1a_u$	17.37	16.19	15.66	5*a*	17.12	15.47	5*b*	16.97	15.82	15.34	$1b_1$	17.26	15.55

[†] EMS experiment [16,17].
[‡] PES experiment [12].
[¶] 1p-GF/ADC(3)/6-311G** calculations [9].
[§] The SOAP/TZ2P model indicates a nearly doubly degenerate orbital but favours $2b_g$ as HOMO.

a more clustered pattern than for the less stable structure of *cis*-butane (D). The same trend is noted for the orbitals of conformations B and C that have a common C_2-axis: the orbitals of the local minimum conformer C are more clustered than those of the B conformation.

3. Outer valence orbital momentum distributions

Conformations of butane exhibit small energy differences, which challenges experiment resolution for their detection. The global minimum structure (A) and the local minimum structure (C) of butane have been observed experimentally [14]. Even though the transition structures B and D have not been identified with current experimental techniques, they play important roles in chemical reactions as they reside along the reaction pathways on the potential-energy surface. Their signatures have, however, been seen in experiments, to be discussed in subsequent sections. Appropriate theoretical methods are important in the study of conformers of organic and biological species. In the conventional coordinate space, the energy-insensitive properties (likely anisotropic properties) such as orbital shape and chemical bonding mechanisms still present challenges to the design of sensitive experimental means of their observation. An example is the claimed application of intense femtosecond laser pulses to derive a tomographic reconstruction of the HOMO of N_2 [40].

Electron-momentum spectroscopy (EMS) in conjunction with quantum-mechanical calculations in momentum space has been a powerful tool to reveal additional information about orbitals including orbital shape and chemical bonding mechanisms of molecules [1,2,6,25–27]. EMS measures directly the binding-energy spectra and individual orbital-momentum distributions (cross sections) [43–44]. DSA [8] was introduced to study the bonding mechanism of molecules and to differentiate electronic structures of conformers [1,2,6,9,27,28] and tautomers [26,41] that exhibit no significant differences in total energy. DSA might also assist interpretation of EMS experiments in decomposition of orbitals in the outer valence shell appearing as clusters due to limited experimental instrumental resolution, evident by a recent joint theory-experimental discovery of tetrahydrofuran [42]. Figure 4 compares the outer valence-orbital MDs of butane conformers, synthesized with the present B3LYP/TZVP//MP2/TZVP model, and the experimental EMS measurements. The orbital MDs, which were simulated based on the experimental conditions at Tsinghua University [16], agree satisfactorily with experiment. The four clusters of orbitals in momentum space exhibit conformation (torsional angle based) related characteristics in the low-momentum region of < 1.0 a.u., whereas in the higher momentum regions, the distributions converge.

As indicated by Wang [8], a small energy splitting of the outer valence orbitals of butane results in experimentally observed orbitals MDs in clusters, due to the large (ca. 1.60 eV) EMS resolution of binding energy spectra. These clusters are gathered according to the binding-energy patterns shown in figure 3. For example, the nine outer valence MOs were clustered into four orbital groups [8] with only the orbital $1a_u$ in the outer valence space being resolved individually. The remaining eight orbitals form three clusters with an orbital MD superposition of $5a_g + 5b_u + 1b_g$, $6b_u + 2a_u$ and the outermost cluster $6a_g + 2b_g + 7a_g$. As is observable in figure 2, orbitals $5b_u$ and $5a_g$ (A, C_{2h}), which are the orbitals with apparent energy discrepancies between theoretical calculations and the PES experiment, are unresolved in EMS. These limitations with current experimental capacity preclude a detailed understanding of the electronic structures. We hence proceed theoretically to decompose the orbital clusters for analysis.

The global minimum structure, anti-butane (A), dominates the outer valence space. Inspection of the outer valence orbital MDs of the experiment and the simulated conformer orbital MDs indicates that the orbitals of the high-energy conformers impose signatures on some clusters. For example, for the "orbital" MDs of the outermost orbital cluster of $7a_g + 2b_g + 6a_g$ (figure 4(a)), even though the anti-butane orbital MDs (solid line) agree with experiment within the error bars, the orbital MDs in the region of momentum greater than 1.0 a.u. obviously fit all the conformers. Moreover, the experimental measurement in the region of small momentum, ≤ 0.2 a.u., exhibits a decreased cross section (figure 4(a)), which might indicate the involvement of other conformers, such as B, C and D, rather than the anti-butane structure A alone. On further rotation of the central C—C bond, A → B → C → D, the next orbital cluster MDs of $2a_u + 6b_u$ (figure 4(b)) show a strongly hybridized feature with an increasing s-component in the region of ≤ 0.5 a.u. It is noted that the EMS measurements produce large error bars in this orbital cluster and no resolved experimental data are available in this region to reflect the complex conformer related properties. The third clustered orbital MDs in figure 4(c) indicate that the experiment measurement produces the orbital MDs of all conformations but likely structure D in very small momentum regions of 0.2 a.u. The only resolved orbital MDs in the outer valence space (figure 4(d)) agree with experiment with respect to structure A.

4. Clustered orbital decomposition

Orbital-based properties become revealed when the clustered "orbital" MD are decomposed. Figure 5 decomposes the outermost cluster of three orbitals for the four conformations, in an orbital symmetry correlated fashion. Figures 4(a) and (c) are a cluster of three orbitals on the outer valence shell, but they behave quite differently as follows. First, the outermost valence orbital cluster MDs split into distinguishable individual conformers in the region of small momentum (figure 4(a)), in contrast with figure 4(c) which does not exhibit apparent

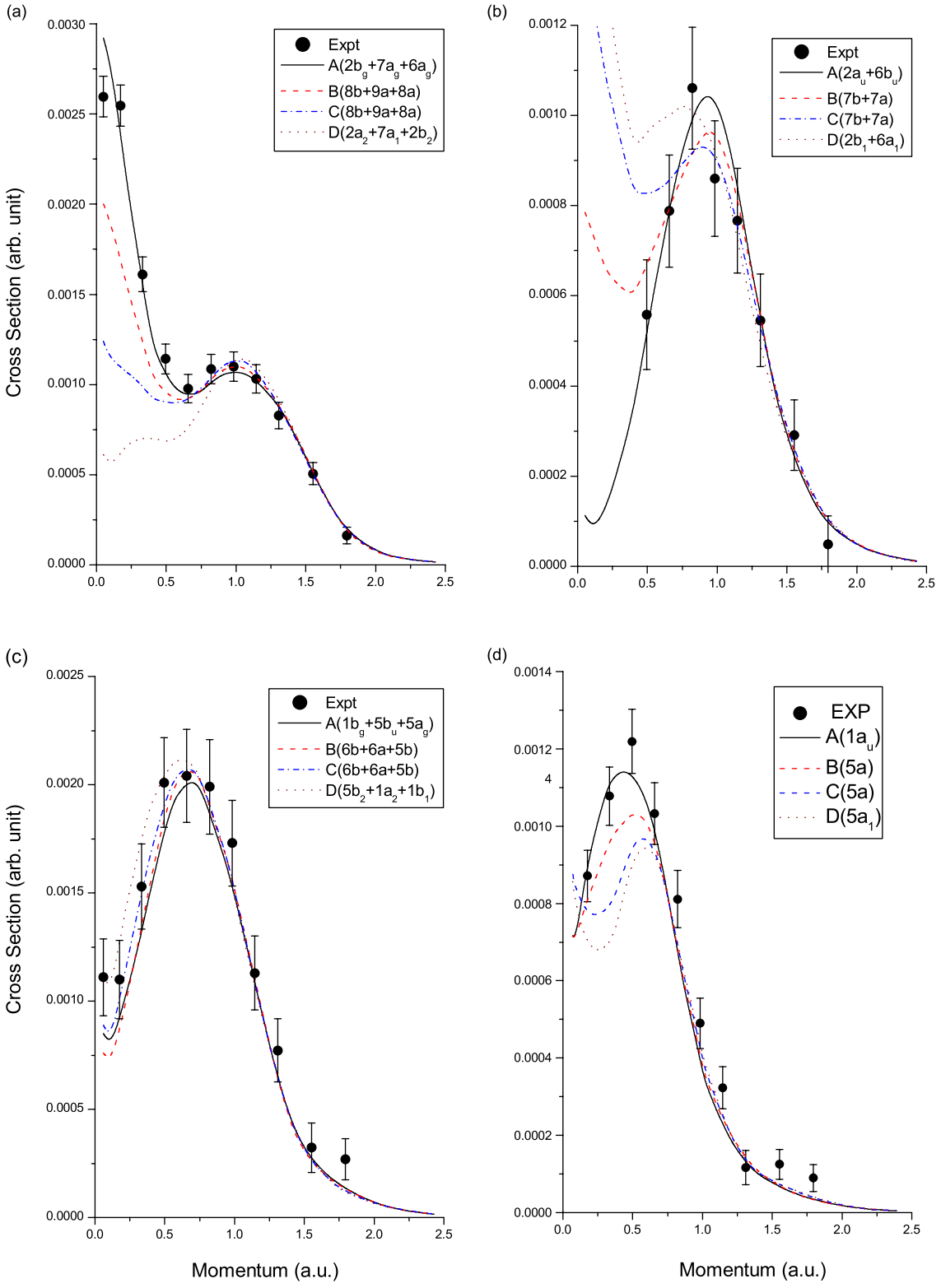

Figure 4. Comparison of EMS experimental [16] orbital MDs in the outer valence shell of anti-butane with synthesized conformer orbital MDs based on the B3LYP/TZVP//MP2/TZVP model and PWIA [43,44].

splitting as a function of torsional motion. Second, the clustered orbital MDs in figure 4(a) indicate the dominance of the global minimum structure A (solid line), whereas the orbital MDs in figure 4(c) favour other conformations such as C (the local minimum gauche butane, dashed and dotted line) and D (the *cis*-butane, dotted line), rather than the most stable structure A. This phenomenon has been observed in the inner valence shell of butane [1] and 1,3-butanediene [2]. Third, the outermost clustered orbital MD display a strong s and p

phase change (figure 4(a)), whereas the cluster of the other trio shows a p dominance.

The decomposed orbital MDs demonstrate disparate orbitally dependent features reflected by their binding energies. In the decomposed orbital MDs in figure 5, the orbitals associated with binding energy 11.57 eV (EMS, table 1) are correlated based on orbital topology given in figure 3. In the decomposed orbital MDs shown in figure 5(b)–(d), the individual orbital MDs split only in the region of small momentum, approximately ≤ 1.0 a.u., which is reflected in the cluster given in figure 5(a), indicating that information in the region of small momentum is sufficiently sensitive to the torsional variation of the conformers. Figure 5(a) indicates that

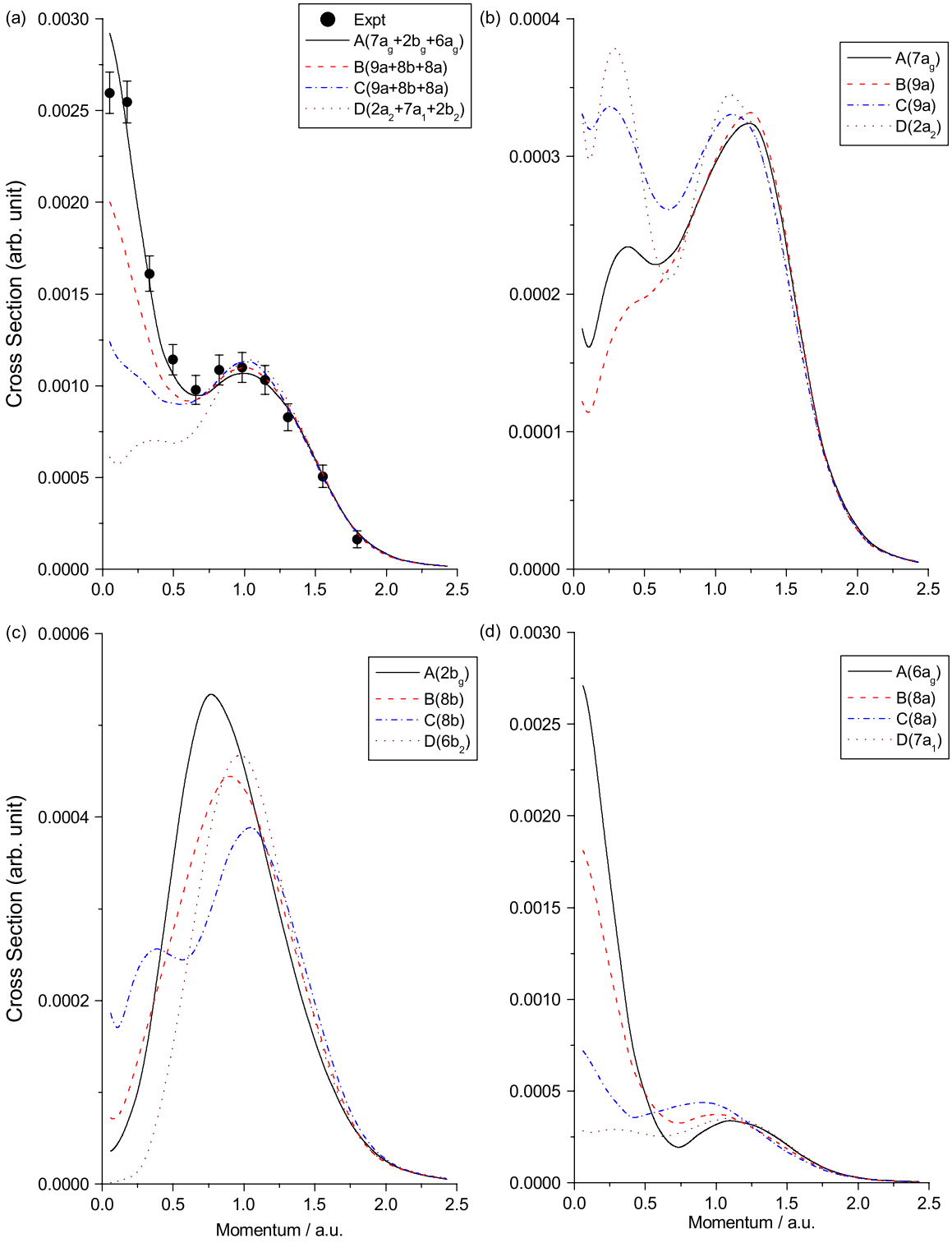

Figure 5. Decomposed orbital MDs (HOMO, MO2 and MO3, A: $7a_g + 2b_g + 6a_g$) of conformers and their clustered orbital MDs, synthesized based on experimental observation.

dominance of structure A in this orbital cluster, the analysis therefore concentrates on the decomposed orbitals of structure A in this cluster (the solid lines). The frontier orbitals of anti-butane (A), HOMO ($7a_g$) and NHOMO ($2b_g$) possess much smaller cross sections in scale than the third orbital ($6a_g$), which indicates that the degree of orbital overlap in HOMO and NHOMO is small, possibly related to the anti-bonding nature. The third orbital exhibits a strong s-component over the p-component, approximately eight times as large, indicating contributions from orbitals containing H_{1s} orbitals.

In the three decomposed orbitals, figure 5(b)–(d), conformers A and B (and likely other conformers with a torsional angle $\leq 90°$) exhibit similarities with the $s^x p^y$ hybridized features in their HOMO ($7a_g$ for A and $9a$ for B). The degree of overlap is small due to local bonds such as C—H as indicated by the intensities. A p-dominant nature in the NHOMO ($2b_g$ for A and $8b$ for B) indicates that the symmetry plane (for A) might serve as a nodal plane. A strong s contribution in the third outermost orbital is shown in figure 5(d). In this orbital ($6a_g$ for A), the p contribution remains almost constant, but the in-plane s-electron contribution is enhanced significantly at small torsional angles. The local bonding overlap is hence larger in this orbital than in the HOMO. Conformations C and D, for which the torsional angle is $\leq 90°$), behave differently. As a "planar" species, the s component in conformer D is strong (dotted lines in figure 5(b)), indicating a larger overlap of the s components in the HOMO ($2a_2$ for D). Similarly, in the third MO (figure 5(d)), the contributions from s and p are balanced, similar to the orbital MDs of HOMOs in C and D. Note that the orbital MD cross section scales are different in (b) and (d). Apart from the cross section indicator, the positions of the phase changes in the orbital MDs reflect the conformational process. The anti-butane conformer A is dominant in this energy region in the spectrum, in agreement with experiment.

The third clustered-orbital MDs also consist of three orbitals, $1b_g + 5b_u + 5a_g$ (for A), but the cluster orbital MDs do not show significant orbital/conformer dependent changes. Figure 6 depicts the decomposed orbitals in momentum space. A distinctive feature of this figure relative to the outermost clustered orbitals is that, in figure 5, the clustered orbitals were dominated by the third orbital of A ($6a_g$) due to its large cross sections, whereas the HOMO and NHOMO were significantly less intense. In figure 6(a), the clustered orbitals also take the approximate distributions of the third orbital in the cluster, i.e. orbital $5a_g$ of A. However, the three orbitals in this cluster exhibit approximately equal intensities of cross sections, as shown in figure 6(b)–(d). What happens in this cluster is that the first and second orbitals, $1b_g$ and $5b_u$ in A, compensate in their shape of cross sections, as displayed in figure 6(b) and (c). Such a significant difference is revealed only when the cluster is fully decomposed.

The other significant difference between this orbital cluster and the outermost orbital cluster is that this cluster is likely dominated by conformers C and D, rather than by the global minimum structure A. Such a phenomenon was discernible for the inner valence shell (orbital $4b$ of conformer C) of butane conformers [1] and the outer valence shell of 1,3-butadiene [2], indicating possible co-existence of rotamers under the experimental conditions. The torsional changes of this cluster have been clearly demonstrated on an orbital base. For example, the first orbital has a clear p-dominant nature for conformer A, indicating a nodal plane. The s electron overlap builds up and becomes separate from the p electrons during rotation (figure 6(b)). In contrast, the in-plane bonding nature of conformer A in orbital $5b_u$ is decreased to allow the localized p electron overlaps to join and to achieve the maximum overlap in conformer D (figure 6(c)). The last orbital in this cluster, $5a_g$(A) − $6a$(B, C) − $1a_2$(D), figure 6(d), is dominated by the p-component in general. The orbital MDs clearly indicate the existence of a particular symmetry related to the central C—C bond in this orbital. The overall orbital MDs of this cluster of three orbitals exhibit that conformer D has the strongest performance in momentum space, although all conformers show similarities in their orbital MDs. The orbital MDs from the EMS experiment are more accurately reproduced by conformers C and D, in particular D as shown in figure 6(a). The PES experimental feature at 15.00 eV in the binding energy spectra [12] supports this observation. The binding energy is 15.09 eV for orbital $1a_2$ of conformer D.

5. Orbital topology and bonding mechanism analysis

All outer valence MOs of the conformers are affected on rotation of the central C—C bond of *n*-butane. The orbital MDs of the conformers reflect such changes through orbital distortion and redistribution of electronic charge. We applied the DSA method [8] to a selected set of outer valence orbitals in order to obtain insight into chemical bonding related to the conformational process of butane. The HOMOs (figure 5(b)) of *n*-butane have been the target of studies of bonding mechanisms and chemical reactions in organic chemistry, as they are typically active and susceptible to changes in chemical processes. The next selected orbital is the set of orbitals $5a_g$(A) − $6a$(B, C) − la_2(D) (figure 6(d)) as this set of orbitals contains a pertinent correlation to the C—C bond rotation. The last orbital "cluster" is the only EMS experimentally resolved orbital in the outer valence shell, i.e. the set of orbitals la_u(A) − $5a$(B, C) − $5a_1$(D) (figure 4(d)).

Figure 7 provides information on the sensitivity of orbital MDs of the HOMO to reflect the distortion of the orbital, with snapshots of redistribution of electronic charge on rotation of the C—C bond. The p-component of the HOMO of conformers experience little variation of their orbital MDs when momentum is >1.25 a.u. What alters significantly is the overlap of s and p

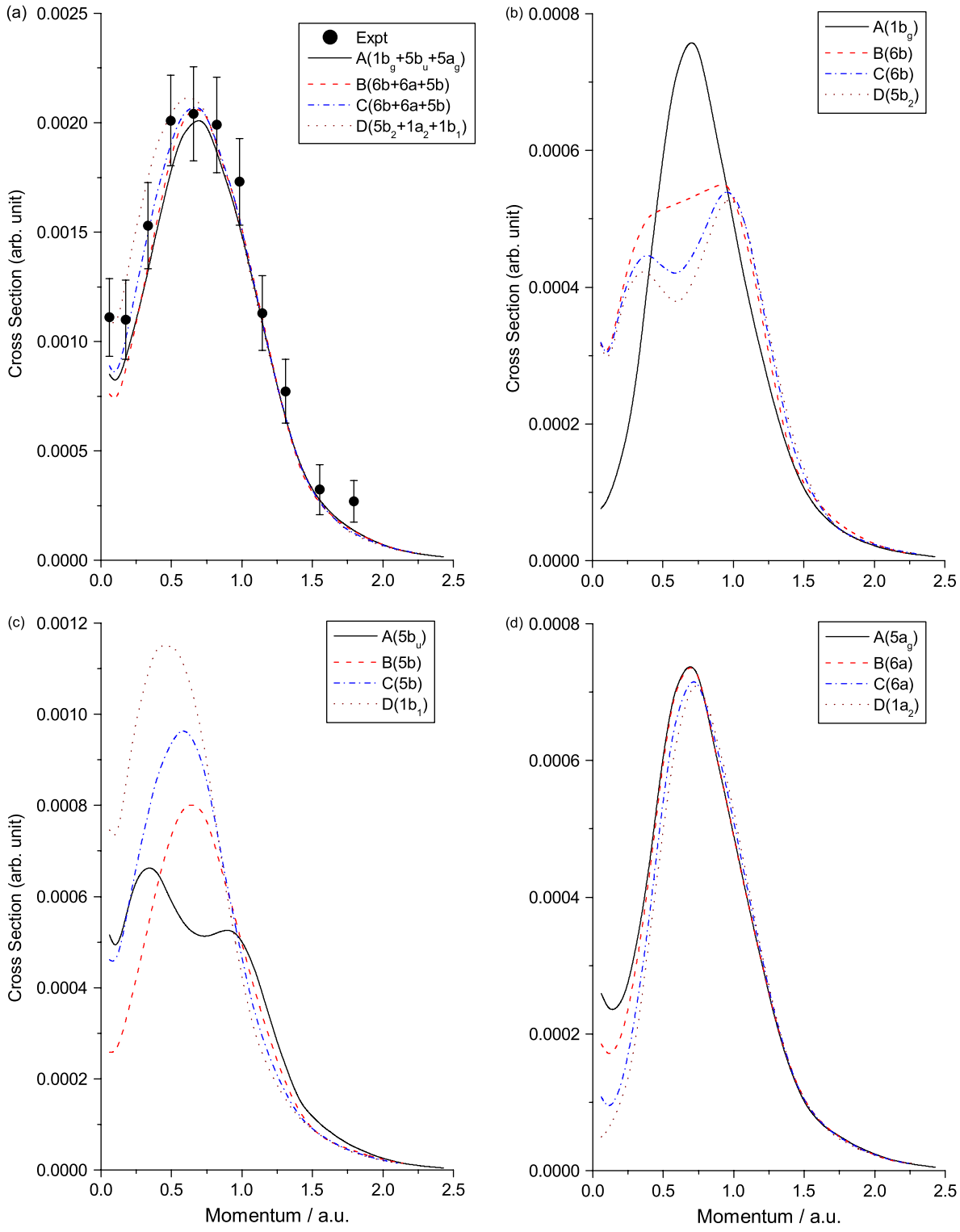

Figure 6. Decomposed orbital MDs (D: $5b_2 + 1a_2 + 1b_1$) of conformers and their clustered orbital MD, synthesized based on experimental observation.

orbitals in the "plane" formed by the carbon atoms (four carbon atoms in A and D but three carbon atoms in B and C). The Dyson orbital charge distributions indicate the p dominant nature of the bonding enhanced by the s electrons of the H atoms connected to the carbons atoms. As the central C—C bond rotation, the overlaps by the p electrons of the carbon atoms in A ($7a_g$) start to distort but still manage to some overlap as seen in B ($9a$). As the rotation continues the overlap (in gray) between the carbon atoms begin to separate until structure D ($2a_2$) is produced. The overlap of electrons between carbons atoms reaches a minimum, in an anti-bonding fashion. The orbital MDs reflect such changes in the small momentum regions in figure 7.

Figure 8 presents interesting orbital MDs of orbital set A($5a_g$) − B($6a$) − C($6a$) − D($1a_2$). The C—C central bond of conformer A is formed from two pairs of terminal C—C bonds on the parallel sides of the Z-shaped conformer in opposite charges, such that the p nature is enhanced by the C—C central bond consisting of the same charges as shown in figure 8 A($5a_g$). The rotation of the central $C_{(1)}$—$C_{(2)}$ bond (approximately 60°) in conformer B reduces such overlap as the four carbon atoms in B are not in the same plane, which causes decreased orbital MDs in the region ≤ca. 0.3 a.u. (dashed line in figure 8). Once the central $C_{(1)}$–$C_{(2)}$ bond rotates beyond 90° to attain conformer C at approximately 120°, the overlapped electron with the same charge "breaks" into three parts so that it further decreases the σ-component in the region of small momentum (refer to C($6a$) in figure 8). When the torsional angle becomes 0° in conformer D ($1a_2$), the "co-planar" symmetry is totally broken in the central C—C region and produces two nodal planes, so that this orbital in D receives a minimized σ-component in the orbital MDs (refer to D($1a2$) in figure 8). The bonding in the $C_{(3)}$–$C_{(1)}$ and $C_{(2)}$–$C_{(4)}$ pairs is only slightly perturbed in the conformational process: their orbital MDs thus remain stable.

With regard to the only EMS experimentally resolved MO ($1a_u$) in the outer valence shell of *n*-butane, figure 9 shows the distributions of orbital electronic charge and corresponding orbital MDs of the conformers, which are correlated as A($1a_u$) − B($5a$) − C($5a$) − D($5a_1$). Conformer A dominates this region of binding energy (approximately 16 eV), as the orbital MDs of this anti-butane conformer agree with the EMS experiment and the

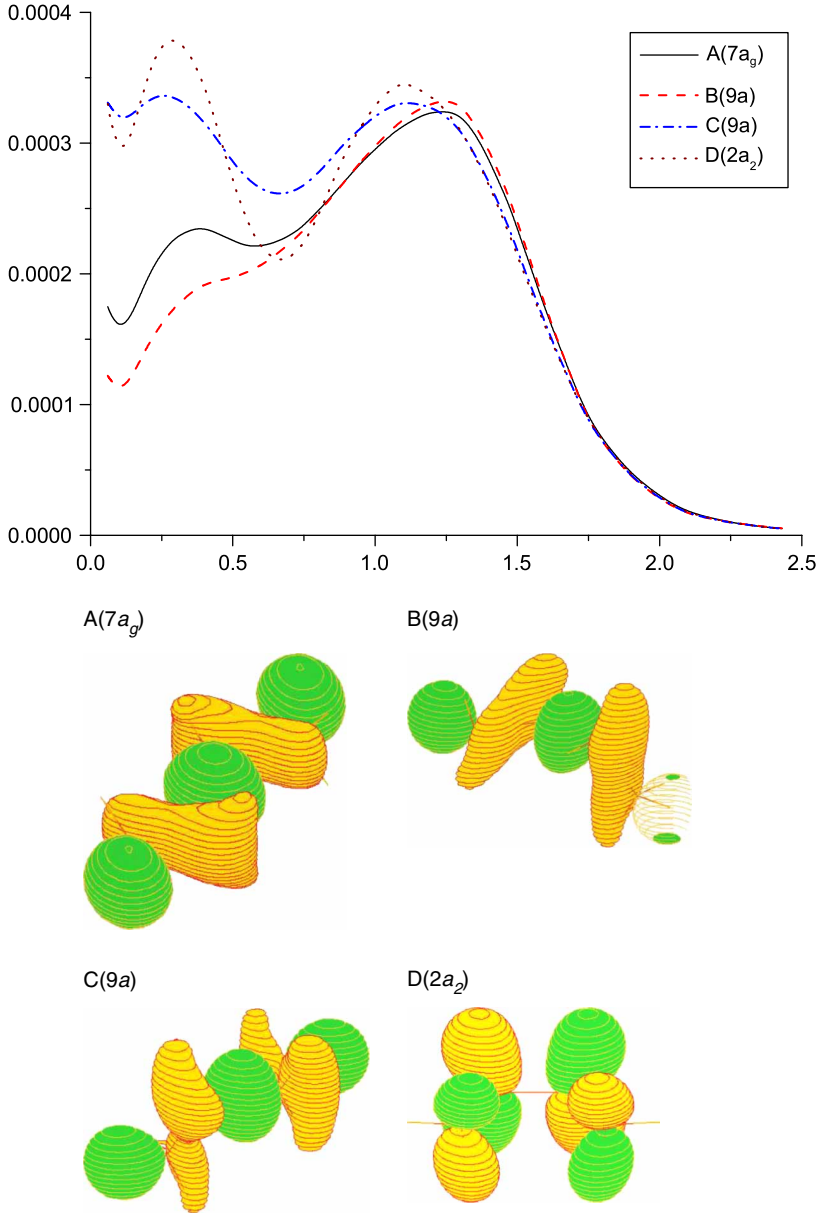

Figure 7. Orbital distortion of HOMO of conformers A–D caused by rotation about the C—C bond in coordinate and momentum space.

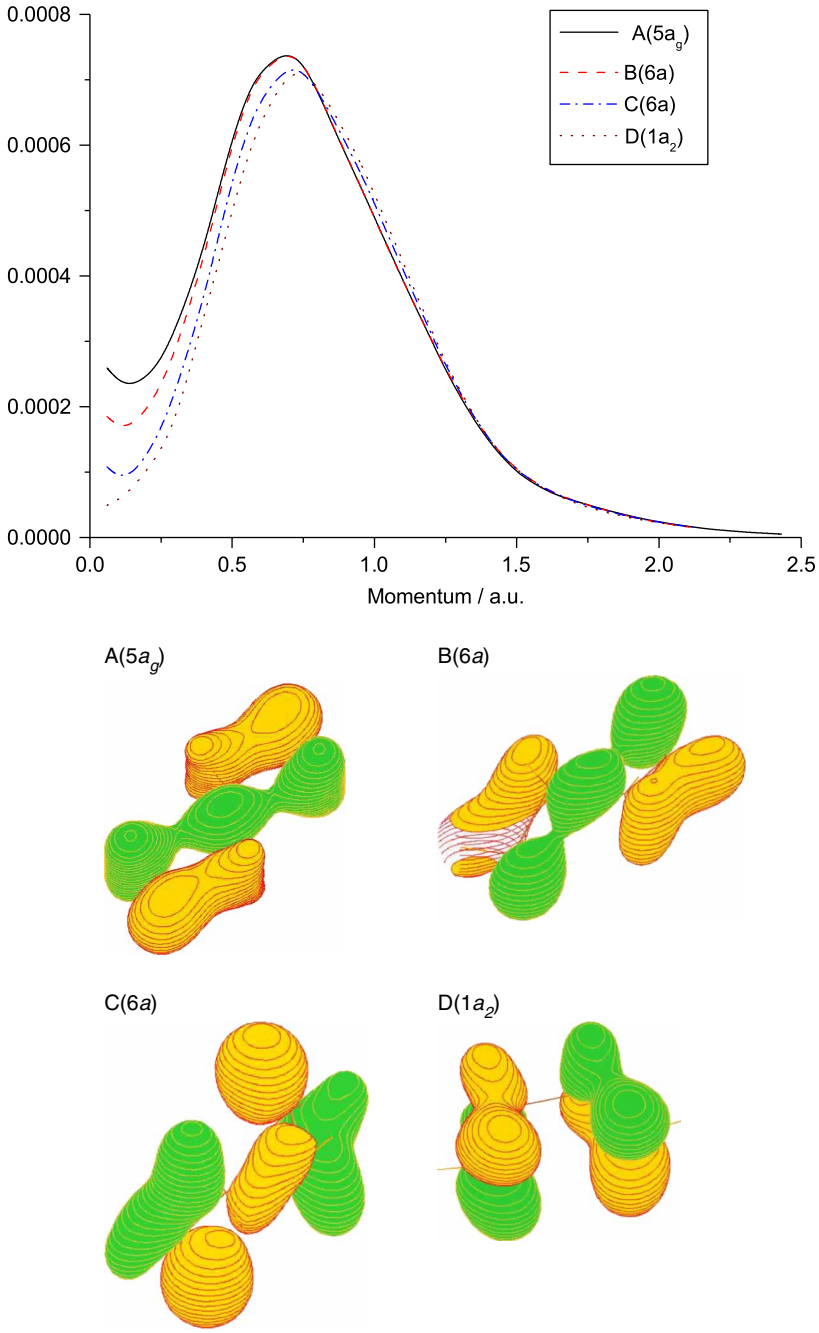

Figure 8. The orbital of conformers "least sensitive" to torsional variation in momentum space in the outer valence shell.

corresponding orbitals of other conformers show no significance in this spectral region. The orbital MDs of the conformers indicate an impact on the bond nature as a result of the orbital distortion. This orbital of anti-butane is an s and p mixed MO dominated by the four carbon $2p_z$ AOs and the 1s AO of the eight out-of-plane hydrogen atoms in a bonding fashion. As a result, this orbital has a nodal plane as the symmetry plane (A, a significant π-bonding character) and at each side of the plane the positive and negative parts of the p_z orbitals have been enhanced by the four out-of-plane 1s hydrogen atoms in a σ fashion bonding (C—H). As the "planar" C_{2h} symmetry of the conformer represents a perfect overlap of the p_z orbitals, the cross sections of this MO are in its maximum overlap position in anti-butane (figure 9 solid line).

As the central C—C bond rotates, for instance to conformer B, the orbital overlap decreases but orbital 5*a* retains roughly one positive and one negative part so that the orbital MD have a decreased intensity but retain one feature (the dashed line) in conformer B. As the C—C bond is rotated beyond 90°, the orbital positive and negative parts are broken into four parts in conformers C and D showing an anti-bonding nature. The isolated CH_2 (the middle carbon atoms) and CH_3 (the terminal carbon atoms) groups involve all 10 hydrogen atoms including the terminal hydrogen atoms. The overlap between the H_{1s}

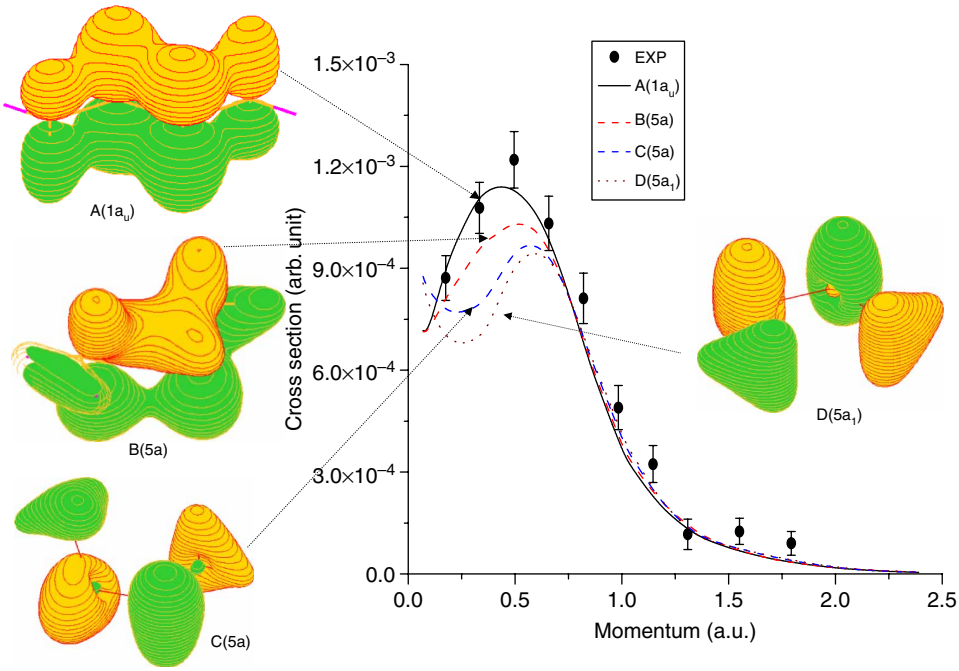

Figure 9. Orbital $1a_u$ (A) of the only EMS experimentally resolved orbital in the outer valence shell of butane.

and Cp_z orbitals within the CH_2 and CH_3 groups slightly increases, whereas the overlap between the groups is largely reduced. This effect is seen in the distributions of electronic charge in conformers C and D. As a result, the integrated single feature in the orbital MDs of conformers A and B splits into two feature and produces a minimum in the orbital MDs of C and D (phase changes). When the torsional angle, δ, attains 180° to produce *cis*-butane (D), the redistributions of electronic charge attain maximum isolation; hence the intensities of the cross sections become further decreased and reach the minimum of the well.

6. Conclusions

We have analysed the orbital topology and bonding mechanism in the outer valence shell of butane using dual-space analysis, in combination with photo-electron spectroscopy and EMS. Calculations indicate that the effects of electron correlation depend on orbitals in the outer valence shell. There is strong evidence in both PES and EMS that some orbitals in the outer valence shell such as orbitals $5b_u$ and $5a_g$ deviate from the global minimum structure, indicating contributions from other conformers in the spectra. In both coordinate space (binding energies) and momentum space (orbitals MDs) the orbital pair $5b_u$ and $5a_g$ is most likely from the conformers C and D of higher energy under the experimental conditions, rather than from the global minimum structure A. The phenomenon has been observed elsewhere [1–4].

In momentum space, the B3LYP/TZVP//MP2/TZVP model reproduces the *n*-butane clustered orbital MDs of experiment in the outer valence space [16]. This work provides details of the orbital topology and orbitals primarily responsible for conformational processes as well as chemical bonding mechanism for butane in its outer valence shell. It has demonstrated that the small momentum region is very sensitive to the conformational changes. As conformers and tautomers exist abundantly in biological molecules, DSA is expected to play an important role in the conformational analysis, a useful alternative to the energy based analysis of specific rotations. The latter unlikely sheds much additional light on the problem [29].

Acknowledgements

The authors acknowledge Australian Research Council (ARC) for an International Linkage Award. FW acknowledges the Australian Partnership for Advanced Computing for using the National Supercomputing Facilities. WNP thanks project 10574079 supported by National Natural Science Foundation of China. Finally, Dr M. Downton is acknowledged for technical assistance.

References

[1] F. Wang, M. Downton. Inner valence shell bonding mechanism of *n*-butane studied using orbital momentum distributions of its conformational isomers. *J. Phys. B At. Mol. Opt. Phys.*, **37**, 557 (2004).

[2] S. Saha, F. Wang, C. Falzon, M.J. Brunger. Coexistence of 1,3-butadiene conformers in ionization energies and Dyson orbitals. *J. Chem. Phys.*, **123**, 124315 (2005).

[3] K.T. Lee, J. Sung, K.J. Lee, Y.D. Park, S.K. Kim. Conformation-dependent ionization energies of L-phenylalanine. *Angew. Chem. Int. Ed.*, **41**, 4114 (2002).

[4] N.J. Kim, G. Jeong, Y.S. Kim, J. Sung, S.K. Kim. Resonant two-photon ionization and laser induced fluorescence spectroscopy of jet-cooled adenine. *J. Chem. Phys.*, **113**, 10051 (2000).

[5] A. Rauk. *Orbital Interaction Theory of Organic Chemistry*, Wiley-Interscience, New York (2001).

[6] M. Downton, F. Wang. Chemical bonding mechanisms of *n*-butane probed by the core molecular orbitals of conformational isomer in *r*-space and *k*-space. *Chem. Phys. Lett.*, **384**, 144 (2004).

[7] N.L. Allinger, J.T. Fermann, W.D. Allen, H.F. Schaefer III. The torsional conformations of butane: Definitive energetics from *ab initio* methods. *J. Chem. Phys.*, **106**(12), 5143 (1997).

[8] F. Wang. Assessment of quantum mechanical models based on resolved orbital momentum distributions of *n*-butane in the outer valence shell. *J. Phys. Chem. A.*, **107**, 10199 (2003).

[9] M.S. Deleuze, W.N. Pang, A. Salam, R.C. Shang. Probing molecular conformations with electron momentum spectroscopy: The case of *n*-butane. *J. Am. Chem. Soc.*, **123**, 4049 (2001).

[10] F. Wang. *n*-Butane–the molecule of the month. October (2004).

[11] J. McMurry. *Organic Chemistry*, 6th ed., Brooks/Cole, New York (2004).

[12] K. Kimura, S. Katsumata, Y. Achiba, T. Yamazaki, S. Iwata. *Handbook of HeI Photoelectron Spectra of Fundamental Organic Molecules*, Japan Scientific Society, Tokyo (1981).

[13] L.S. Cederbaum, J. Schirmer, W. Domcke, W. von Niessen. *J. Am. Chem. Soc.*, **116**, 10715 (1994).

[14] W.A. Herrebout, B.J. van der Veken, A. Wang, J.R. Durig. Enthalpy difference between conformers of *n*-butane and the potential function governing conformational interchange. *J. Chem. Phys.*, **99**, 413 (1995).

[15] G. Bieri, F. Burger, E. Heilbronner, J.P. Maier. Valence ionization energies of hydrocarbons. *Helv. Chim. Acta.*, **60**, 2213 (1977).

[16] W. Pang, R. Shang, N. Gao, W. Zhang, J. Gao, J. Deng, X. Chen, Y. Zheng. Measurements of valence orbital momentum profiles of *n*-butane by a high-resolution (e, 2e) spectrometer. *Phys. Lett. A*, **248**, 230 (1998).

[17] W. Pang, R. Shang, J. Gao, N. Gao, X. Chen, M. Dueleze. Investigation of the valence electronic structure of *n*-butane using (e, 2e) spectroscopy. *Chem. Phys. Lett.*, **296**, 605 (1998).

[18] L. Deng, T. Zieger. Combined density functional theory and intrinsic reaction coordinate study on the conrotatory ring-opening of cyclobutene. *J. Phys. Chem.*, **99**(2), 612 (1995).

[19] J.K. Deng, G.Q. Li, J.D. Huang, H. Deng, X.D. Wang, F. Wang, Y. He, Y.A. Zhang, C.G. Ning, N.F. Gao, Y. Wang, X.J. Chen, Y. Zheng, C.E. Brion. The valence shell binding energy spectra and frontier orbital momentum profiles of methylpropane (isobutane) by binary (e, 2e) spectroscopy. *Chem. Phys. Lett.*, 313(1–2), 134 (1999).

[20] I. Flamant, D.H. Mosley, M. Dueluze, J.M. Andre, J. Delhalle. Dependence of the electronic structure on the chain geometry in stereoregular polypropylene: An exploratory theoretical study. *Int. J. Quantum Chem.*, **52**, 469 (1994).

[21] A.S. Duwez, S. Di Paolo, J. Ghijsens, J. Riga, M. Deleuze, J. Delhalle. Surface molecular structure of self-assembled alkanethiols evidenced by UPS and photoemission with synchrotron radiation. *J. Phys. Chem. B*, **101**, 884 (1997).

[22] P. Duffy, D.P. Chong, M.E. Casida, D.R. Salahub. Assessment of Kohn-Sham density-functional orbitals as approximate Dyson orbitals for the calculation of electron-momentum-spectroscopy scattering cross-sections. *Phys. Rev. A*, **50**, 4707 (1994).

[23] F. Wang, M.J. Brunger, D.A. Winkler. Structural impact on the methano bridge in norbornadiene, norbornene and norbornane. *J. Phys. Chem. Solids*, **65**, 2041 (2004).

[24] B. Herrera, O. Dolgounitcheva, V.G. Zakrzewski, A. Toro-Labbe, J.V. Ortiz. Conformational effects on glycine ionization energies and Dyson orbitals. *J. Phys. Chem. A*, **108**, 11703 (2004).

[25] F. Wang, M.J. Brunger, I.E. McCarthy, D.A. Winkler. Exploring the electronic structure of 2,6-stelladione from momentum space I: the p-dominant molecular orbitals in the outer valence shell. *Chem. Phys. Lett.*, **382**, 217 (2003).

[26] F. Wang, M. Downton, N. Kidwani. Adenine tautomer electronic structural signatures studied using dual space analysis. *J. Theor. Comput. Chem.*, **4**, 247 (2005).

[27] C. Falzon, F. Wang. Understanding glycine conformation through molecular orbitals. *J. Chem. Phys.*, **123** (2005).

[28] M.S. Deleuze, W.N. Pang, A. Salam, R.C. Shang. Probing molecular conformations with electron momentum spectroscopy: the case of *n*-butane (J. Am. Chem. Soc., **123**, 4049 (2001)). *J. Am. Chem. Soc.,* **125**, 15683 (2003).

[29] K.B. Wiberg, P.H. Vaccaro, J.R. Cheeseman. Conformational effects on optical rotation. 3-Substituted 1-butenes. *J. Am. Chem. Soc.*, **125**, 1888 (2003).

[30] K.B. Wiberg, Y.G. Wang. Conformational energies for 2-substituted butanes. *J. Comput. Chem.*, **25**, 1127 (2004).

[31] M.W. Schmidt, K.K. Baldridge, J.A. Boatz, S.T. Elbert, M.S. Gordon, J.H. Jensen, S. Koseki, N. Matsunaga, K.A. Nguyen, S.J. Su, T.L. Windus, M. Dupuis, J.A. Montgomery. *J. Comput. Chem.*, **14**, 1347 (1993).

[32] N. Godbout, D.R. Salahub, J. Andzelm, E. Wimmer. Optimization of Gaussian-type basis-sets for local spin-density functional calculations. 1. Boron through neon, optimization technique and validation. *Can. J. Chem.*, **70**, 560 (1992).

[33] O.V. Gritsenko, R. van Leeuman, E.J. Baerends. Analysis of electron interaction and atomic shell structure in terms of local potentials. *J. Chem. Phys.*, **101**, 8955 (1994).

[34] O.V. Gritsenko, R. van Leeuman, E.J. Baerends. Self-consistent approximation to the Kohn-Sham exchange potential. *Phys. Rev. A*, **52**, 1870 (1995).

[35] O.V. Gritsenko, P.R.T. Schipper, E.J. Baerends. Approximation of the exchange-correlation Kohn-Sham potential with a statistical average of different orbital model potentials. *Chem. Phys. Lett.*, **302**, 199 (1999).

[36] D.P. Chong, O.V. Gritsenko, E.J. Baerends. Interpretation of the Kohn-Sham orbital energies as approximate vertical ionization potentials. *J. Chem. Phys.*, **116**, 1760 (2002).

[37] O.V. Gritsenko, B. Braïda, E.J. Baerends. Physical interpretation and evaluation of the Kohn-Sham and Dyson components of the epsilon-I relations between the Kohn-Sham orbital energies and the ionization potentials. *J. Chem. Phys.*, **119**, 1937 (2003).

[38] O. Dolgounitcheva, V.G. Zakrzewski, J.V. Ortiz. Electron propagator theory of guanine and its cations: Tautomerism and photoelectron spectra. *J. Am. Chem. Soc.*, **122**, 12304 (2000).

[39] D.P. Chong, E. Van Lenthe, S. van Gisbergen, E.J. Baerends. Even-tempered slater-type orbitals revisited: From hydrogen to krypton. *J. Comput. Chem.*, **25**, 1030 (2004).

[40] J. Itatani, J. Levesque, D. Zeidler, H. Nikura, H. Pepin, J.C. Kieffer, P.B. Corkum, D.M. Villeneuve. Tomographic imaging of molecular orbitals. *Nature*, **432**, 867 (2004).

[41] S. Saha, F. Wang, C. Falzon, M. J. Brunger. Coexistence of 1,3-butadiene conformers in ionization energies and Dyson orbitals. *Mol. Simul.*, **32**, 1261 (2006).

[42] T.C. Yang, G.L. Su, C.G. Ning, J.K. Deng, F. Wang, S.F. Zhang, X.G. Ren, Y.R. Huang. New diagnostic of the most populated conformer of tetrahydrofuran in the gas phase. *J. Phys. Chem. A*, **111**, 4297 (2007).

[43] I.E. McCarthy, E. Weigold. Electron momentum spectroscopy of atoms and molecules. *Rep. Prog. Phys.*, **54**, 789 (1991).

[44] E. Weigold, I.E. McCarthy. *Electron Momentum Spectroscopy*, Kluwer-Academic, Dordrecht, New York (1999).